Nuclear Instruments and Methods in Physics Research B 287 (2012) 130–134

Contents lists available at SciVerse ScienceDirect

Nuclear Instruments and Methods in Physics Research B

journal homepage: www.elsevier.com/locate/nimb

The irradiation effects of $Gd_2Hf_2O_7$ and $Gd_2Ti_2O_7$

Y.H. Li [a,b,*], J. Wen [a], Y.Q. Wang [b], Z.G. Wang [c], M. Tang [b], J.A. Valdez [b], K.E. Sickafus [b]

[a] School of Nuclear Science and Technology, Lanzhou University, Lanzhou 730000, China
[b] Materials Science and Technology Division, Los Alamos National Laboratory, Los Alamos, NM 87545, USA
[c] Institute of Modern Physics, Chinese Academy of Sciences, Lanzhou 730000, China

ARTICLE INFO

Article history:
Received 19 April 2012
Received in revised form 24 May 2012
Available online 21 June 2012

Keywords:
$Gd_2Ti_2O_7$
$Gd_2Hf_2O_7$
Ion irradiation effects

ABSTRACT

In this report, we present dramatically different behavior between isostructural $Gd_2Hf_2O_7$ and $Gd_2Ti_2O_7$ pyrochlore using 400 keV Ne^{2+} irradiation under cryogenic conditions (~77 K), in which the lattice volume of the irradiated layer of $Gd_2Ti_2O_7$ increased with ion fluence up to 1×10^{15} ions/cm^2, whereas, the lattice volume of the irradiated layer of $Gd_2Hf_2O_7$ decreased with increasing fluence from 1×10^{15} to 6×10^{16} ions/cm^2. The cation radius ratio r_A/r_B, the bond-type of A–O and B–O bonds, the order-to-disorder transition energy of $Gd_2Hf_2O_7$ and $Gd_2Ti_2O_7$, temperature–composition (T–C) phase diagrams of HfO_2–Gd_2O_3 and TiO_2–Gd_2O_3 mixtures were used to explain the response of $Gd_2Hf_2O_7$ and $Gd_2Ti_2O_7$ to ion irradiation-induced structure transformation.

1. Introduction

Pyrochlore materials, with the general formula $A_2B_2O_7$, where A and B are metallic cations that can either be trivalent and tetravalent or divalent and pentavalent, represent an important structure type for immobilization of actinide-rich wastes and inert matrices [1–7]. In recent years, some papers have been published on ion irradiation effects of rare-earth titanate pyrochlores ($A_2Ti_2O_7$, A = Y, and Sm–Lu) with different lanthanide elements occupying the A sites [5–7]. The response of Ti pyrochlores to radiation-induced amorphization is almost not dependent on the cations at the A sites. All these Ti pyrochlores are sensitive to ion irradiation and can be amorphized at a relatively low fluence [4]. On the other hand, the response behaviors of rare-earth Zr pyrochlores ($A_2Zr_2O_7$, A = Y, and La–Gd) to radiation-induced amorphization are much different from each other when the A cations are different. Certain compositions readily disorder into the defect fluorite structure upon ion irradiation, and therefore they are remarkably resistant to amorphization. For example, $Gd_2Zr_2O_7$ do not experience a radiation-induced transformation from crystalline to amorphous state even at a peak ballistic damage dose as high as ~36 displacements per atom (dpa). On the other hand, $La_2Zr_2O_7$ can be amorphized at a relatively low ion dose of ~5.5 dpa for 1.5 MeV Xe^+ ion irradiations at room temperature [8]. Theoretically studies showed that the major factors that can influence the response of pyrochlores to ion irradiation-induced amorphization include the cation radius ratio of A cation over B cation [1], defect formation energies on the stability of pyrochlore [3], electronic structures of A-site cations [9,10], and A–O_{48f} and A–O_{8b} bonds [11]. Studies of Sickafus et al. indicated that T–C diagram is a good indicator to predict the irradiation tolerance of complex oxides systematically [3]. It was suggested that the compounds with natural order-to-disorder (O–D) transformations have good tolerance to ion irradiation induced amorphization.

Although extensive ion irradiation studies have been conducted on Ti and Zr pyrochlores, so far, only a few experimental investigations have been performed on ion irradiation effects of hafnate pyrochlores ($A_2Hf_2O_7$), where the B-site cation ionic radius of Hf^{4+} (0.71 Å) is between those of Ti^{4+} (0.605 Å) and Zr^{4+} (0.72 Å) [12]. In this paper, we compare, for the first time, the irradiation effects of $Gd_2Hf_2O_7$ and $Gd_2Ti_2O_7$ isostructural pyrochlores. Their response to the irradiation is discussed in terms of ionic sizes of the cations, the bond-type of A–O and B–O bonds, the order-to-disorder transition energy of $Gd_2Hf_2O_7$ and $Gd_2Ti_2O_7$, and the temperature–composition (T–C) phase diagrams of HfO_2–Gd_2O_3 and TiO_2–Gd_2O_3 mixtures.

2. Experimental procedure

Polycrystalline $Gd_2Ti_2O_7$ and $Gd_2Hf_2O_7$ samples were synthesized from Gd_2O_3 (Alfa Aesar, 99.99% purity), HfO_2 and TiO_2 powers (Aldrich Chemical company, 99.99% purity), by conventional ceramic processing procedures. The measured densities of the sintered pellets were larger than ~90% of their theoretically densities.

Ion irradiation was performed under cryogenic condition ($T_{substrate}$ ~77 K) at the Ion Beam Materials Laboratory, Los Alamos National Laboratory, using a 200 kV Danfysik high current research ion implanter. The 400 keV Ne^{2+} ions were implanted at normal

* Corresponding author at: School of Nuclear Science and Technology, Lanzhou University, Lanzhou 730000, China.
E-mail address: liyuhong@lzu.edu.cn (Y.H. Li).

0168-583X/$ - see front matter © 2012 Elsevier B.V. All rights reserved.
http://dx.doi.org/10.1016/j.nimb.2012.06.003

incidence at fluences ranging from 5×10^{14} to 6×10^{16} ions/cm^2 using an ion flux of $\sim 1 \times 10^{12}$ ions/cm^2 s. The projected range of the 400 keV Ne ions in $Gd_2Ti_2O_7$ and $Gd_2Hf_2O_7$ were estimated using the Monte Carlo code SRIM [13]. The projected range, R_p, was estimated to be 411 ± 125 and 369 ± 134 nm, respectively (with a target density $\rho = 6.567$ g/cm^3 of $Gd_2Ti_2O_7$ and $\rho = 8.95$ g/cm^3 of $Gd_2Hf_2O_7$). In these calculations, we assumed the threshold displacement energies for Gd, Ti, Hf and O are all 40 eV (these energies are arbitrary assumptions because we currently do not have experimental or theoretical estimates for these values) [14,15].

Grazing Incidence X-ray Diffraction (GIXRD) was used to characterize the crystal structure of the pristine and ion irradiated samples using a Bruker AXS D8 advanced X-ray diffractometer, θ–2θ geometry, Cu–Kα radiation, and the X-ray incidence angle $\gamma = 0.5°$. The depths of the X-rays in $Gd_2Ti_2O_7$ and $Gd_2Hf_2O_7$ at $\gamma = 0.5°$are 89 and 75 nm, respectively. The X-ray penetration depths were estimated geometrically [16]. The step size of the scan angle was 0.02° and a dwell time of 4 s per step. The scan range was 10–75°.

3. Results and discussion

Fig. 1 shows GIXRD patterns obtained from the pristine $Gd_2Hf_2O_7$ and the $Gd_2Hf_2O_7$ irradiated with 400 keV Ne^{2+} ions at fluences of 1.0×10^{15}–6.0×10^{16} ions/cm^2, corresponding to a peak ballistic damage dose of ~0.25–15 dpa. The $Gd_2Hf_2O_7$ samples exhibit a weakly ordered pyrochlore structure: only three fundamental pyrochlore diffraction peaks of P{111}, P{113} and P{331} with small number counts can be discerned, diffraction peaks of P{222}, P{400}, P{440} and P{622} (or F{111}, F{200}, F{220} and F{311}) are fundamental fluorite reflections, which are contributed by both diffraction of pyrochlore structure and fluorite structure. From Fig. 1, one can discern the following phenomena: The three fundamental pyrochlore diffractions of P{111}, P{113} and P{331} diminished for the irradiated $Gd_2Hf_2O_7$. All fluorite peaks shift towards larger 2θ with increasing Ne ion fluence from 1×10^{15} to 6×10^{16} ions/cm^2. As an example, P{222} peak was zoomed on in Fig. 1, showing the gradual displacement with increasing Ne ion fluence. The displacement of the lattice reflections to larger 2θ is indicative of unit cell contraction.

Fig. 2 shows GIXRD patterns obtained from pristine $Gd_2Ti_2O_7$ and $Gd_2Ti_2O_7$ irradiated with 400 keV Ne^{2+} ions at fluences of 5.0×10^{14}–1.0×10^{15} ions/cm^2, corresponding to a peak ballistic damage dose of ~0.16–0.32 dpa. The samples exhibit a pyrochlore superlattice structure. All peaks shift towards smaller 2θ with increasing Ne ions. The displacement of the lattice reflection peaks to smaller 2θ indicates unit cell swelling. That is to say, the lattice parameter of the irradiated $Gd_2Ti_2O_7$ increases with increasing Ne ion fluence.

In order to quantify the changes of the lattice parameter of $Gd_2Ti_2O_7$ and $Gd_2Hf_2O_7$ with Ne ion fluence, Table 1 summarizes lattice parameter of the pristine and the irradiated $Gd_2Ti_2O_7$ and $Gd_2Hf_2O_7$. All data in Table 1 were calculated by using XRD data of $Gd_2Ti_2O_7$ and $Gd_2Hf_2O_7$ pellets before irradiation and after irradiation at $\gamma = 0.5°$ X-ray incident angle. In Table 1, d-spacings were calculated according to Bragg's law, $2d \cdot \sin\theta = n\lambda$, and the lattice parameter a was calculated using individual reflection indices $\{hkl\}$ and the cubic unit cell relationship $a = d_{hkl}(h^2 + k^2 + l^2)^{1/2}$. Four fundamental fluorite reflections P{222}, P{400}, P{440} and P{622} were used to calculate the average lattice parameter. From the lattice parameter value obtained for a given fluence, the changes of lattice parameter were determined as $\Delta a = a - a_0$, where a_0 is the lattice parameter of each pristine, unirradiated $Gd_2Ti_2O_7$ and $Gd_2Hf_2O_7$, while a is the lattice parameter of each irradiated $Gd_2Ti_2O_7$ and $Gd_2Hf_2O_7$. According to the previous study of ion irradiation effects on $Y_2Ti_2O_7$ pyrochlore, the lattice change is not a constant; the calculation result of lattice parameter is an average value, $\langle a \rangle$ [14]. From Table 1, the average lattice parameter changes of $Gd_2Ti_2O_7$ and $Gd_2Hf_2O_7$ were opposite. For $Gd_2Ti_2O_7$, the average lattice parameter increased with increasing fluence from 5×10^{14} to 1×10^{15} ions/cm^2, and it was amorphized when the irradiated fluence reached 1×10^{16} ions/cm^2 with the corresponding peak ballistic damage dose of 3.2 dpa (there is no attempt to show the TEM image here). Whereas for $Gd_2Hf_2O_7$, the average lattice parameter decreased with increasing dose from 1×10^{15} to 6×10^{16} ions/cm^2. The irradiated $Gd_2Hf_2O_7$ transformed to a disor-

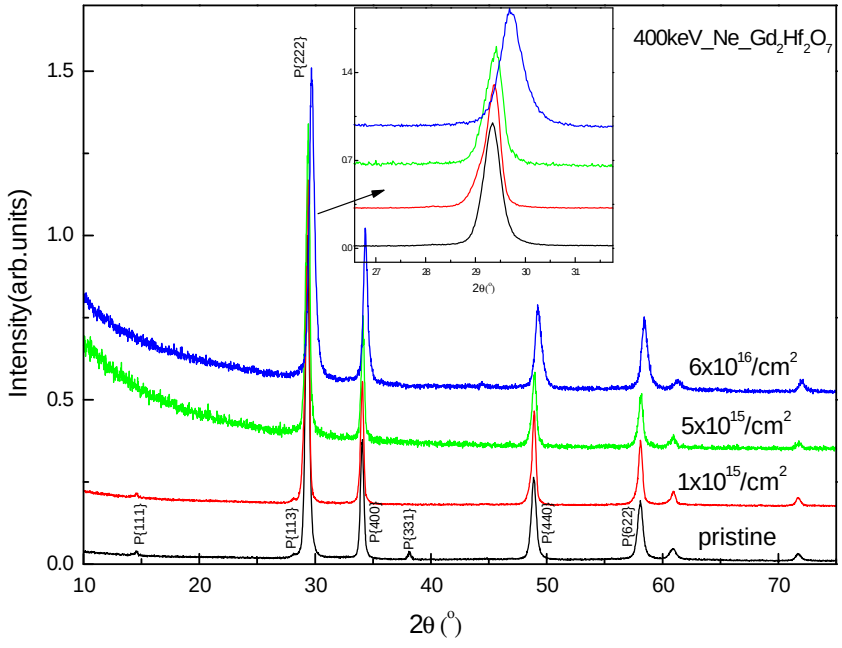

Fig. 1. GIXRD patterns obtained from un-irradiated and irradiated $Gd_2Hf_2O_7$ samples to a fluence of 1×10^{15}–6×10^{16} ions/cm^2 at X-ray incidence angle of 0.5°. The inserted diagram was the zoomed in P{222} peak.

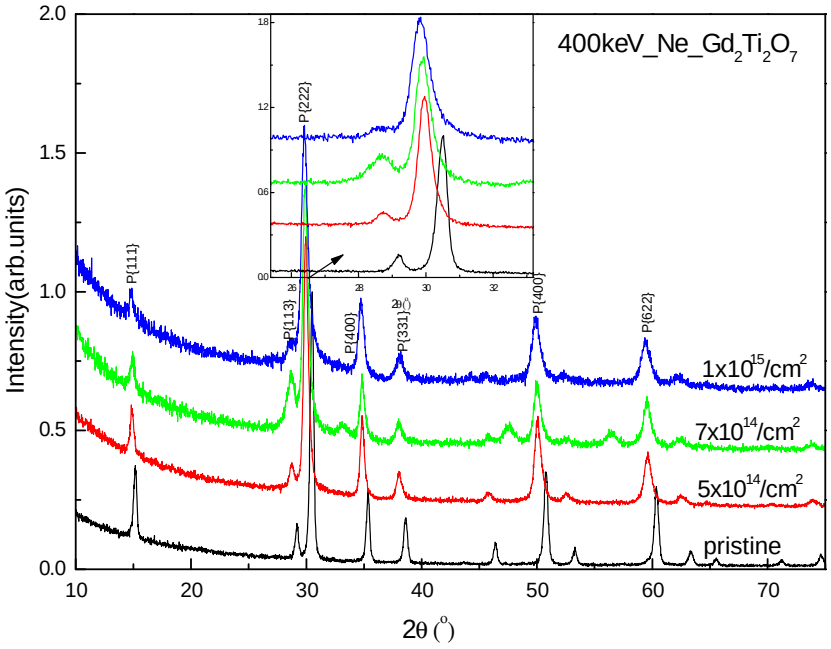

Fig. 2. GIXRD patterns obtained from un-irradiated and irradiated $Gd_2Ti_2O_7$ samples to a fluence of 5×10^{14}–1×10^{15} ions/cm^2 at X-ray incidence angle of 0.5°. The inserted diagram was the zoomed in P{222} peak.

Table 1
Experimental results for lattice parameter and volume change in $Gd_2Hf_2O_7$ and $Gd_2Ti_2O_7$, as a function of Ne ion irradiation fluence, based on four main XRD peaks of pyrochlore P{222}, P{400}, P{440} and P{622}.

Dose (ions/cm^2)	$Gd_2Hf_2O_7$				$Gd_2Ti_2O_7$			
	a or a_0(Å)	V_0 or V(Å^3)	ΔV(Å^3)	$\Delta V/V_0$(%)	a(Å)	V_0 or V(Å^3)	ΔV(Å^3)	$\Delta V/V_0$(%)
Pristine	10.5288	1167.178	0	0	10.1542	1046.977	0	0
5×10^{14}	No experimental data				10.2990	1092.409	45.432	4.34
7×10^{14}					10.3049	1094.288	47.311	4.52
1×10^{15}	10.5228	1165.178	−2.0	−0.17	10.3066	1101.638	54.661	5.22
1×10^{16}	10.5118	1161.533	−5.6	−0.48	Amorphous			
6×10^{16}	10.4420	1138.555	−28.62	−2.45				

dered fluorite structure as proved by the disappearance of the pyrochlore superlattice reflections P{111}, P{113} and P{331}. No evidence of amorphization was observed for $Gd_2Hf_2O_7$ even at a high ion fluence of 6×10^{16} ions/cm^2 (~15 dpa).

The dramatically different behavior of $Gd_2Ti_2O_7$ and $Gd_2Hf_2O_7$ under ion irradiation showed striking opposite differences in lattice parameter and resistance to amorphization. $Gd_2Ti_2O_7$ swelled and was amorphized readily, whereas $Gd_2Hf_2O_7$ contracted and could not be amorphized even at 15 dpa. Similar example involves the dramatic difference in irradiation resistance between $Er_2Ti_2O_7$ and $Er_2Zr_2O_7$, with $Er_2Ti_2O_7$ is readily amorphized while $Er_2Zr_2O_7$ remains crystalline even at very high doses [1]. Another research indicated that $La_2Zr_2O_7$ pyrochlore is more resistant than structurally identical $La_2Hf_2O_7$ pyrochlore [17]. The radiation response of pyrochlore is highly dependent on composition and has previously been interpreted as being related to the radius ratio, r_A^{3+}/r_B^{4+}, of the A- and B-site cations. The compounds with more similar cation radius are more likely to form as disordered fluorites than as ordered pyrochlore, and fluorites are inherently more radiation resistant than pyrochlores [1]. So, $Gd_2Hf_2O_7$, with an ionic radius ratio of $r_A^{3+}/r_B^{4+} = 1.48$, would more likely disorder to the defect fluorite structure than $Gd_2Ti_2O_7$ ($r_A^{3+}/r_B^{4+} = 1.74$) [12]. Therefore, $Gd_2Hf_2O_7$ is more resistant to amorphization than $Gd_2Ti_2O_7$ under ion irradiation.

Another factor that plays an obvious and important role in determining the radiation response is the bond-type of A–O and B–O bonds [9,18]. According to the Mulliken overlap population analysis by Lumpkin et al. [19], the covalency of Ti–O bond is larger than that of Hf–O. This trend also roughly follows that of Pauling's electronegativity. The electronegativity of Hf (1.3) is much smaller than that of Ti (1.54). The fact that Ti–O bond is more covalent than Hf–O bond may also explain why $Gd_2Ti_2O_7$ is more difficult to disorder than $Gd_2Hf_2O_7$ [18]. As the disordered structure is usually more resistant to the radiation damage [3], it is quite natural to understand that $Gd_2Hf_2O_7$ is more resistant to radiation than induced amorphization $Gd_2Ti_2O_7$.

First-principle calculations suggested that defect formation energy of order-to-disorder transition also plays an important role in determining the stability of radiation-induced amorphization of pyrochlore [9,10,20]. Pyrochlores with high defect formation energy will not easily relax back to the pyrochlore structure once defects are formed by either ion irradiation or high-pressure, and therefore the compounds behave less robust in a radiation environment [20,21]. Chao et al. calculated the disordering energies of $A_2B_2O_7$ (A^{3+} = Er, Dy, Tb, Gd and B^{4+} = Zr, Hf, Ti, Sn) using first-principle, they found that for the same A^{3+} cation, the disordering energies increase in the order $A_2Sn_2O_7 > A_2Ti_2O_7 > A_2Hf_2O_7 > A_2Zr_2O_7$ (A = Er, Dy, Tb and Gd)[18]. So, as compared to $Gd_2Ti_2O_7$, the defects in $Gd_2Hf_2O_7$ are easily formed. The weakly ordered pyrochlore $Gd_2Hf_2O_7$ structure has a strong propensity to transformation to the disordered-fluorite structure.

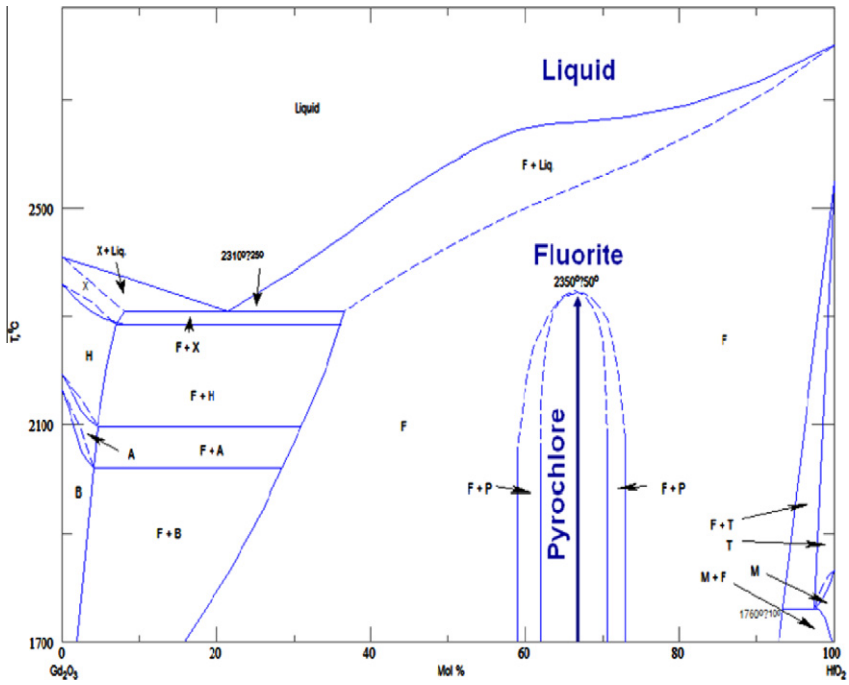

Fig. 3. Temperature–composition (T–C) phase diagram for Gd_2O_3–HfO_2 binary oxide mixtures (based on the T–C phase diagram in [22]). The vertical line in the diagram denotes the composition of $Gd_2Hf_2O_7$.

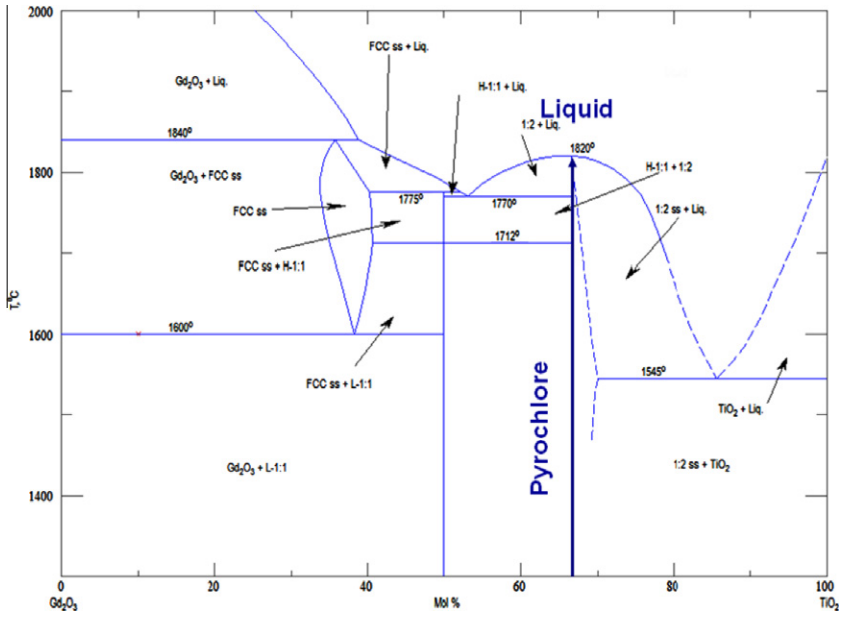

Fig. 4. Temperature–composition (T–C) phase diagram for Gd_2O_3–TiO_2 binary oxide mixtures (based on the T–C phase diagram in [23]). The vertical line in the diagram denotes the composition of $Gd_2Ti_2O_7$.

Previous ion irradiation experiment on derivate fluorite showed that a structure which has a strong propensity to accommodate ion-induced defects should have a high resistance to amorphization [3]. For example, $Dy_4Zr_3O_{12}$ cannot be amorphized even at very high radiation dose (55 dpa) because $Dy_4Zr_3O_{12}$ is initially a disordered fluorite. Whereas, titanate pyrochlores are far more susceptible to radiation-induced amorphization because titanates cannot readily accommodate disorder (the amorphous dose is less than 0.5 dpa). That is to say, disorder in titanates is energetically costly [14]. Our previous study indicates that the temperature–composition (T–C) phase diagram of compound is a good indicator that can directly reflect the structural tolerance to the irradiation induced order-to-disorder (O–D) transformation. Figs. 3 and 4 show the T–C phase diagrams of HfO_2–Gd_2O_3 and TiO_2–Gd_2O_3 mixtures, respectively [22,23]. The $Gd_2Ti_2O_7$ pyrochlore is stable before it melts. While for 2:2:7 $Gd_2Hf_2O_7$ pyrochlore, it transforms to a disordered fluorite phase with increasing temperature before melt. For disordered fluorite $Gd_2Hf_2O_7$, Hf and Gd cations are randomly arranged on the cation sites, oxygen ions and oxygen vacancies are randomly arranged on the anion sites. Thus, it is reasonable to understand the experimental results: $Gd_2Ti_2O_7$ is amorphized at low ion irradiation fluence, whereas $Gd_2Hf_2O_7$

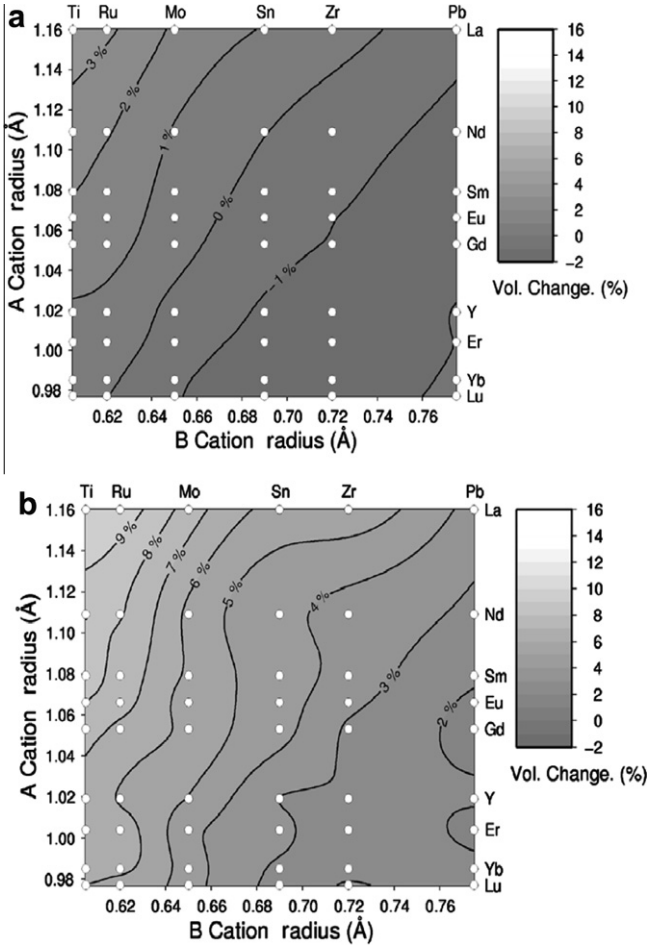

Fig. 5. Volume change associated with irradiation process (a) pyrochlore to fluorite, (b) pyrochlore to amorphous [25].

transforms to a disordered fluorite and shows remarkable resistance to amorphization under ion irradiation.

In addition, the volume changes associated with different A and B cations of $A_2B_2O_7$ structural transition from pyrochlore to fluorite, pyrochlore to amorphous were generated by Rushton et al., using molecular dynamics, as shown in Fig. 5(a) and (b), respectively [24]. The volume changes from pyrochlore to fluorite reported in Fig. 5(a) suggest that for $Gd_2Zr_2O_7$ the transformation from pyrochlore to fluorite is accompanied by a volume compaction of about 1%. This was also confirmed by the ion irradiation experiments in $Gd_2Zr_2O_7$ [25]. However, for $Gd_2Ti_2O_7$ the transformation from pyrochlore to amorphous as shown in Fig. 5(b), there is a significant volume expansion of about 7–8%. Although the volume change of $Gd_2Hf_2O_7$ from pyrochlore to fluorite transformation was not calculated, it can be deduced from Fig. 5(a) that there is also a volume compaction effect on $Gd_2Hf_2O_7$ under ion irradiation. The conclusion is based on the following facts: $Gd_2Hf_2O_7$ undergoes an order-to-disorder transformation from pyrochlore to fluorite when exposed to ion irradiation according to T-C phase diagram of $Gd_2Hf_2O_7$; meanwhile, the main structural transformation in $Gd_2Hf_2O_7$ under ion irradiation within the maximum fluence of 6×10^{16} ions/cm^2 is pyrochlore-to-fluorite transformation as shown in Fig. 1. So Fig. 5(a) can be used to explain the volume changes of $Gd_2Hf_2O_7$ after ion irradiation. From Fig. 5(a), the pyrochlore-to-fluorite change in $Gd_2Sn_2O_7$ is also accompanied a volume compaction a little smaller than 1%. The radius of Hf^{4+} is 0.72 Å, which is larger than that of Sn^{4+} (0.69 Å) but only slighter smaller than that of Zr^{4+} (0.73 Å). Therefore, the volume also decreases due to the pyrochlore-to-fluorite transformation in $Gd_2Hf_2O_7$, as in $Gd_2Zr_2O_7$.

4. Conclusions

In summary, hafnate pyrochlore $Gd_2Hf_2O_7$ is found to be more radiation tolerant than its titanate equivalent $Gd_2Ti_2O_7$ because $Gd_2Hf_2O_7$ is more similar to the parent fluorite phase. On the other hand, other factors such as ionic radius ratio and bond-type of A- and B-site cations, defect formation energy of cations and anions also play a role in the ion irradiation effect of these compounds. The experimental observation reported here is consistent with previous predictions: a structure that has a strong propensity to accommodate ion-induced defects should have a high resistance to amorphization. Volume changes of the irradiated $Gd_2Hf_2O_7$ and $Gd_2Ti_2O_7$ are consistent with the theoretical prediction from atomic scale computer simulations.

The results from the current study further confirm that the T–C phase diagram, the ionic radius ratio and bond-type of A- and B-site cations, the O–D fluorite defect reaction pair energy are good indicators to judge potential high radiation tolerance ceramic compounds for the immobilization of high-level nuclear waste and excess nuclear materials.

Acknowledgements

This work was supported by the National Natural Science Foundation of China (11175076, 10975065, 91026021 and 11135002). The work also was sponsored by the U.S. Department of Energy (DOE), Office of Basic Energy Sciences (OBES).

References

[1] K.E. Sickafus, L. Minervini, R.W. Grimes, J.A. Valdez, M. Ishimaru, F. Li, K.J. McClellan, T. Hartmann, Science 289 (2000) 748.
[2] W.J. Weber, A. Navrotsky, S. Stefanovsky, E.R. Vance, E. Vernaz, MRS Bull. 34 (2009) 46.
[3] K.E. Sickafus, R.W. Grimes, J.A. Valdez, A. Cleave, M. Tang, M. Ishimaru, S.M. Corish, C.R. Stanek, B.P. Uberuaga, Nat. Mater. 6 (2007) 217.
[4] B.D. Begg, N.J. Hess, W.J. Weber, R. Devanathan, J.P. Icenhower, S. Thevuthasan, B.P. McGrail, J. Nucl. Mater. 288 (2001) 208.
[5] R.C. Ewing, W.J. Weber, J. Lian, J. Appl. Phys. 95 (2004) 5949.
[6] J. Chen, J. Lian, L.M. Wang, R.C. Ewing, Appl. Phys. Lett. 79 (2001) 1989.
[7] M. Lang, F. Zhang, J.M. Zhang, J.W. Wang, J. Lian, W.J. Weber, B. Schuster, C. Trautmann, R. Neumann, R.C. Ewing, Nucl. Instr. Meth. B 268 (2010) 2951.
[8] J. Lian, X.T. Zu, K.V.G. Kutty, J. Chen, R.C. Ewing, Phys. Rev. B 66 (2002) 054108.
[9] H.Y. Xiao, X.T. Zu, F. Gao, W.J. Weber, J. Appl. Phys. 104 (2008) 073503.
[10] N. Li, H.Y. Xiao, X.T. Zu, L.M. Wang, R.C. Ewing, J. Lian, F. Gao, J. Appl. Phys. 102 (2007) 063704.
[11] J. Lian, R.C. Ewing, L.M. Wang, J. Mater. Res. 19 (2005) 1575.
[12] R.D. Shannon, Acta Crystallogr., Sect. A: Cryst. Phys. Diffr. Theor. Gen. Crystallogr., 32 (1976) 751.
[13] J.F. Ziegler, J.P. Biersack, U. Littmark, The Stopping and Range of Ions in Matter (SRIM). Available from: <http://www.srim.org>.
[14] J. Zhang, Y.Q. Wang, J.A. Valdez, M. Tang, K.E. Sickafus, Nucl. Instr. Meth. B 419 (2011) 396.
[15] Y.H. Li, B.P. Uberuaga, C. Jiang, S. Choudhury, J.A. Valdez, M.K. Patel, J. Won, Y.Q. Wang, M. Tang, D.J. Safarik, D.D. Byler, K.J. McClellan, I.O. Usov, T. Hartmann, G. Baldinozzi, K.E. Sickafus, Phys. Rev. Lett. 108 (2012) 195504.
[16] D. Rafaja, V. Valvoda, A.J. Perry, J.R. Treglio, Surf. Coat. Technol. 92 (1997) 135.
[17] G.R. Lumpkin, K.R. Whittle, S. Rios, K.L. Smith, N.J. Zaluzee, J. Phys.: Condens. Matter 16 (2004) 8557.
[18] C. Jiang, C.R. Stanek, K.E. Sickafus, B.P. Uberuaga, Phys. Rev. B 79 (2009) 104203.
[19] G.R. Lumpkin, M. Pruneda, S. Rios, K.L. Smith, K. Trachenko, K.R. Whittle, N.J. Zaluzec, J. Solid State Chem. 180 (2007) 1512.
[20] F.X. Zhang, J.W. Wang, J. Lian, M.K. Lang, U. Becker, R.C. Ewing, Phys. Rev. Lett. 100 (2008) 045503.
[21] J. Lian, R.C. Ewing, L.M. Wang, K.B. Helean, J. Mater. Res. 19 (2004) 1575.
[22] A.V. Shevchenko, L.M. Lopato, L.V. Nazerenko, Izv. Akad. Nauk SSSR Neorg. Mater. 20 (11) (1984) 1862.
[23] J.L. Waring, S.J. Schneider, J. Res. Natl. Bur. Stand. Sec. A 69 (3) (1965) 255.
[24] M.J.D. Rushton, C.R. Stanek, A.R. Cleave, B.P. Uberuaga, K.E. Sickafus, R.W. Grimes, Nucl. Instr. Meth. B 255 (2007) 151.
[25] M.K. Patel, V. Vijayakumar, D.K. Avasthi, S. Kailas, J.C. Pivin, V. Grover, B.P. Mandal, A.K. Tyagi, Nucl. Instr. Meth. B 266 (2008) 2898.